Tellus (1977), *29*, 484–501

The sensitivity of response of climatic characteristics in a two-level general circulation model to small changes in solar radiation

By H. B. GORDON[1] and D. R. DAVIES, *Exeter University, Department of Mathematics, North Park Road, Exeter EX4 4QE, UK*

(Manuscript received July 6, 1976; in final form January 1, 1977)

ABSTRACT

A two-level, quasi-geostrophic, β-plane, general circulation model is developed, incorporating a time-dependent surface energy balance equation and a time-dependent heating function at the 500 mb level, with an associated feedback relationship. This system enables the surface temperature distribution to be evaluated as a function of time in the model, and so allows an associated variable spatial distribution of surface albedo to be carried in the model, including a simulated "snow and ice" edge. The effect on the model of successive small changes in solar radiation (of ½% up to a total of 3%) are then studied by carrying out numerical experiments over long time periods, these being sufficiently long (involving a total time of integration of 1800 model days) to produce oscillations in model heating and albedo distributions about asymptotic mean values. The successive latitudinal positions of the, zonally averaged, "snow and ice" edge agree approximately with those calculated by Gordon and Davies (1974) using a modified form of the statical energy balance method of Budyko (1969). However, the experiments also showed that the greater the reduction made in solar radiation the greater was the ensuing amplitude of spatial movement of the associated albedo distribution, implying a strong tendency towards instability of the simulated edge as the reduction approached a value of 3%.

1. Introduction

During recent years there has been a widespread and speculative discussion concerning the effects on climate of, e.g. sun-spot periodicity, volcanic dust veils, changes in the earth's orbit and man's production of industrial heat and pollution. However, whatever may be the quantitative effects of these external forcing factors on the broad scale patterns of atmospheric flow, the fundamental atmospheric link is the feedback relationship between atmospheric heating (or cooling) and the dynamics of the atmospheric flow systems (measured by the flow patterns at various heights and interpreted incisively in recent years through applications of the concepts of zonal and eddy kinetic and potential energies). A deeper understanding of this basic link has in recent years been obtained through extensive numerical experiments using general circulation models. If reasonably accurate predictions of climatic change are ever to be achieved and a quantitative expression constructed to describe speculative suggestions concerning changes in external forcing factors, it will undoubtedly be through continued development of these models and statistical extrapolations based on their dynamical structures.

Excellent reviews of the problems involved in the development of climate models have recently been published, e.g. by Smagorinsky (1974), Schneider & Dickinson (1974) and Gal-chen & Schneider (1976). As indicated in these reviews, a hierarchy of models is being used to advance understanding; these range in complexity from the statical energy balance systems, initiated by Budyko (1969), to high resolution dynamical models. Each type of model development has its place in seeking an understanding of the contribution to planetary scale processes of the primary physical factors associated with each temporal and spatial scale resolved by the model, and each has its own

[1] Now at the Australian Numerical Meteorology Research Centre, Melbourne, Australia.

particular disadvantages. The high resolution systems carry the disadvantage of requiring highly detailed parameterizations of phenomena on many spatial and temporal scales (not all fully understood as yet, in depth); they also require heavy and expensive computer usage, with the associated difficulty of coping properly (in a numerical and a physical sense) with the effect of growth of grid-point errors and also errors due to the requirement of accurate model specification of phenomena on scales below the grid spacing threshold. The simple statical energy balance prediction systems have the disadvantage of not including time variations in the essential dynamics, such as baroclinic instability wave structures or the consequences of, e.g. large-scale barotropic instability. Prediction in the sense of accurate climate forecasting is not yet in view, but prediction of the consequences of changes in external conditions on general dynamical characteristics is now feasible; in particular, light can now be thrown on the basic question of sensitivity of a climate state to changes in the primary external factor, i.e. solar radiation.

Additionally, in the development of a sequence of models a good appreciation of the consequences of change in a given external factor is obtained, if the computed characteristics agree in two models incorporating different levels of complexity. This was done, e.g. in a numerical experiment described in a brief note by Gordon & Davies (1975). In this experiment, a two-level, time-dependent general circulation model was used to predict the changes in latitudinal position of a zonally averaged simulated "ice–snow" edge (defined in terms of the surface albedo) following small changes in solar radiation. The results were found to be roughly similar, up to 3% reductions in solar radiation, to those computed from a modified form of the statical energy balance, Budyko (1969) method. The important question was also considered of stability of the "ice–snow" edge, which cannot be studied through the medium of a statical model. It was found that there was a tendency for climatic instability (expressed in terms of the calculated spatial amplitude of oscillation of the simulated ice–snow edge) to increase as a 3% reduction in solar heating was approached.

The object of the present paper is to describe the details of the model constructed to obtain this result and some of the detailed analyses made. The main new feature of the model is a feedback relationship between the model 500 mb temperature and the model surface temperature. In addition, it is suggested that the results of the very long time period integrations may be related to the general question of transitivity or intransitivity of climate, within the limitations of a relatively simple general circulation model. Sudden changes in jet stream behaviour, with barotropic instability characteristics, were also observed at several hundred days' separation in a long time integration of 1800 days.

2. The basic model

The general circulation model used is a modified form of the one experimented with by Everson & Davies (1970), which is basically a Phillips (1956) type of quasi-geostrophic, β-plane system. The advantage of using this type of relatively simple model is of course that the very long time integrations needed in a study of climatic change become feasible. The disadvantage is that many important features of the real atmosphere are not explicitly represented and are only implicitly featured in the model mechanism through the use of many climatological observed values. A major difficulty in the model is that, although baroclinic instability growth and decay are variable with position around the β-plane equivalent of latitude, basic empirical coefficients concerning atmospheric and terrestrial radiation and basic features of a surface energy balance equation are taken as *averages* around latitude circles. Consequently, the strong differential heating (and topographic effect) between land and sea is smoothed out, although the smoothing does include a fixed latitudinally varying representation of heat transfer between atmosphere and sea. Nevertheless, the model, since it is time-dependent, does give a first-order estimate of the stability, or otherwise, of spatial oscillations in surface albedo distribution (simulating approximately a "snow–ice edge") for differing solar radiation values: this is difficult to assess using statical energy balance methods. Comparison of mean zonal positions of a "snow–ice edge" with results obtained with the latter method, strengthens (or otherwise) confidence in the energy balance method predictions. Similarly, comparison of results with a subsequent, properly differentiated, land–sea model will give us insight into the relative contribution of this important effect in influencing sensitivity of a given climatic state. This is a valid method of obtaining an understanding of this problem; it is an alternative to the method of developing complex high resolution systems simulating in as much detail as possible, present day climatic conditions. The disadvantages of the latter method, of course, lie in (a) requiring excessive computation to carry out the required series of numerical experiments, (b) requiring also exact representation of highly detailed smaller scale phenomena which are not as yet fully understood.

The work of model development fell into two stages. Firstly, computer techniques and choice of optimum parameterization coefficients were studied in a model with a geographically fixed heating function at 500 mb. Secondly, this restriction of a fixed heating function is removed by the use of an atmospheric heating parameterization together with a surface energy balance equation. This enables the model to predict surface and 500 mb temperatures, and to carry a feedback relationship between them. The varying surface temperature distribution carries with it a surface albedo distribution, simulating in a rough way a "snow–ice edge", but of course, at this stage in our model development the model does not contain a detailed sea–ice dynamical structure.

The domain of spatial integration is a β-plane representation of a hemispherical surface in which heating representations of tropical and polar regions are included in order to provide available potential energy, creating a large-scale flow system through positive correlation of non-adiabatic heating and variations in temperature. The dissipation mechanisms included are simple parameterizations of surface drag and internal (vertical) eddy shearing stresses due to "free atmosphere" turbulence, and of sub-grid scale lateral "diffusive" eddy stresses. No thermal vertical eddy transfer effects are included, consistent without assumption of constant static stability. Thermal energy is supplied to the model through a thermodynamic equation applied at 500 mb; dynamical equations are applied at the 750 mb and 250 mb levels. A two-parameter prediction scheme is used, defined by the geostrophic stream function ψ and the relative potential vorticity q. The prognostic equations can be expressed in the forms (1) and (2) and the diagnostic equations by (3) and (4) applying a conventional notation as used by Phillips (1956). In these equations, suffixes 1 and 3 refer to model levels at 250 mb and 750 mb respectively, λ is a measure of static stability, k_2 is an internal tur-

$$\frac{\partial q_1}{\partial t} = -\mathbf{V}_1 \cdot \nabla(\beta y + q_1) + A\nabla^2 q_1 - \frac{R\lambda^2}{f_0 c_p}\dot{Q}_2 - k_2[q_1 - q_3 + 2\lambda^2(\psi_1 - \psi_3)] \quad (1)$$

$$\frac{\partial q_3}{\partial t} = -\mathbf{V}_3 \cdot \nabla(\beta y + q_3) + A\nabla^2 q_3 + \frac{R\lambda^2}{f_0 c_p}\dot{Q}_2 + k_2[q_1 - q_3 + 2\lambda^2(\psi_1 - \psi_3)] - \frac{k_4}{2}[3q_3 - q_1 - 4\lambda^2(\psi_1 - \psi_3)] \quad (2)$$

$$q_1 = \nabla^2\psi_1 - \lambda^2(\psi_1 - \psi_3) \quad (3)$$

$$q_3 = \nabla^2\psi_3 + \lambda^2(\psi_1 - \psi_3) \quad (4)$$

bulent (vertical) stress coefficient at level 2 (500 mbs), k_4 is a surface stress coefficient at level 4. Horizontal Laplacian type terms, $A\nabla^2 q$, for momentum and $A\nabla^2 T$ for heat, are included to represent sub-grid scale lateral eddy diffusion, taking the coefficients A to be the same for momentum and heat. The term $\dot{Q}_2$ represents the non-adiabatic rate of heating at level 2; this is initially held constant at a given latitude during a series of numerical experiments to determine optimum numerical values of the parameterization coefficients and optimum numerical techniques for the model. It is then allowed to vary with time and position over very long integration periods, by introducing a dependence on the predicted 500 mb temperature and on the surface temperature through a surface heating condition. The model temperature, T_2, at 500 mb is given from (1) to (4) by $f_0(\psi_1 - \psi_3)/R$.

The $\dot{Q}_2$ dependence on latitude, θ, chosen for the initial integration was an adapted form of that used by Everson & Davies (1970). They modified the empirical heating function tabled by Smagorinsky (1963; Table A5 and Fig. A5) by multiplying those values by a geometric factor cos θ, so that heating on a β-plane was approximately equivalent to that on a sphere: these values are shown in Fig. 1, A, and satisfy the condition that the planetary mean heating is zero. However, this distribution suffers from the disadvantage of having a maximum cooling at a latitude away from the pole. Numerical experiments with the model were then found to lead to a relatively inactive region near the pole and to give rise to model temperatures attaining their

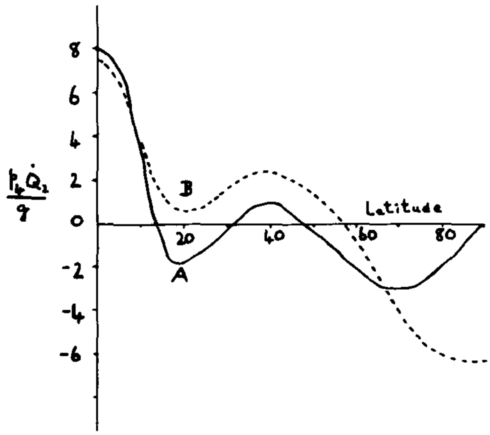

Fig. 1. Non-adiabatic heating function, $\dot{Q}_2$, at level 2 in $\mathrm{Jkg^{-1}\ sec^{-1}}$ units, as a function of latitude; as used in the preliminary computation: ——, initially tested, A; – – – – finally used, B.

lowest values away from the pole, and so displacing the centre of action of the baroclinic wave southwards. Since the main investigation was aimed at a study of the model changes of surface albedo in the high latitude ice-covered zone, a more realistic latitudinal distribution of heating was sought which would give rise to enhanced activity in the β-plane polar flows. From the Smagorinsky data it may be verified that the hemispheric mean of the heating is very nearly zero, as expected. In order to allow for the disparity between the β-plane geometry and that of the hemisphere, it is necessary to adjust the heating values obtained through the Smagorinsky heating formulation in accordance with the requirement for a zero mean heating in the time independent case. This is accomplished in the manner displayed in Fig. 1, curve B, and is similar to the heating parameterization used at the lower levels of the 4-level β-plane model of Searle & Davies (1975). Full details of the method are given by Gordon (1975). This procedure was found to be satisfactory in producing a more active polar region and was used for the main integrations.

For the major part of the integrations, this constraint of a time independent heating was removed by using the heating outlined for use in a two-level model by Smagorinsky (1963). In order to simulate a moving albedo distribution it is necessary to allow the model to predict a surface temperature distribution, T_*, to which such a distribution can be attached, using available empirical values. To achieve this a relationship between T_2 (expressed in eqs. (1) to (4)) and T_* has to be formulated. This can be done by using the formulation described by Smagorinsky using the same notation.

A surface energy balance equation (expressed in the notation used by Smagorinsky) gives one relationship between T_* and T_2; this is

$$\sigma T_*^4 = S_* + \nu_\downarrow \sigma T_2^4 - E_s - E_L - M \tag{5}$$

where σ is the Stephan–Boltzmann constant, $S_*(\theta)$ is the solar radiation absorbed by the surface, $\nu_\downarrow(\theta)$ is the downward atmospheric transmission parameter taken at 500 mb, $E_s(\theta)$ and $E_L(\theta)$ are respectively the flux of sensible and latent heat of evaporation from the surface to the atmosphere and $M(\theta)$ is the flux divergence of heat in the oceans, and transferred to the atmosphere, due to lateral transport. $S_*(\theta)$, $\nu_\downarrow(\theta)$, $E_s(\theta)$, $E_L(\theta)$, $M(\theta)$ are all taken as zonal and annual averages and empirical values are tabulated by Smagorinsky. A second relationship between T_* and T_2 in terms of $\dot{Q}_2$ is given by expressing the heating rate per unit area of a vertical column of the atmosphere; we obtain

$$\frac{p_4}{g}\dot{Q}_2 = S_a + \Gamma\sigma T_*^4 - (\nu_\downarrow + \nu_\uparrow)\sigma T_2^4 + E_s + C \tag{6}$$

where $S_a(\theta)$ is solar radiation absorbed by the atmosphere, $\Gamma(\theta)$ is long wave absorptivity of a whole vertical column of atmosphere, $\nu_\uparrow$ is an upward transmissive parameter for atmospheric long wave radiation, at 500 mb, $C(\theta)$ is latent heat of condensation. Using (5) and (6) we then obtain the negative feedback relation

$$\frac{p_4}{g}\dot{Q}_2(\theta,\lambda,t) = A(\theta,\lambda,t) - \mu(\theta)\sigma T_2^4(\theta,\lambda,t) \tag{7}$$

used in the second stage of our numerical experiments:

$$A(\theta,\lambda,t) = S_a + E_s + C + \Gamma(S_* - E_s - E_L - M),$$
$$\text{and } \mu(\theta) = \nu_\uparrow + (1-\Gamma)\nu_\downarrow$$

As the integration proceeds, changes in the T_* distribution carry an associated surface albedo distribution, A_*, linked through the data tabled by

Smagorinsky. This influences the S_* distribution through the equation (Smagorinsky, 1963, equation, A2),

$$S_*(\theta, \lambda, t) = [1 - A_*(\theta, \lambda, t)](1 - \chi)(1 - A_a)S_0 \quad (8)$$

where $\chi(\theta)$ is the opacity of the atmosphere for solar radiation, A_a is the atmosphere's albedo, $S_0(\theta)$ is the solar radiation at the top of the atmosphere, χ, A_a, and S_0 are assumed known from observational data. Changes in S_* then relate back to $\dot{Q}_2$ through eq. (7).

3. Numerical techniques and parameterization coefficient values

As discussed, e.g. by Searle & Davies (1975), the choice of "optimum" numerical values for the coefficients appearing in parameterization of various physical processes poses a very large problem in the running of any numerical model atmosphere. Order of magnitude values can be deduced from observed data and an optimum set of values found for a given model by numerical experiments. The method used for determining the initial heating function was described in Section 2. The other parameters to be quantified in the model relate to static stability and to horizontal and vertical sub-grid turbulent stresses. It should of course be noted that the latter also describe in a numerical model a smoothing effect arising out of growth of grid point numerical errors. Thus the choice of numerical techniques of integration and choice of parameterization coefficients taken together have to be made for a particular model to satisfy some given criteria. In our numerical experiments these are taken to be (a) eddy kinetic energy variations with time to simulate general characteristics of observed data, (b) surface synoptic flow patterns to simulate general characteristics of observed patterns.

The horizontal spatial extent of the β-plane integration area was taken to be 9000 km, East–West, with a grid resolution of 375 km and 9687.5 km, North–South, with a grid spacing of 312.5 km. The numerical integration was carried out in two stages as in previous Phillips type models. In the first stage the equations are limited to zonal averages and are maintained describing a zonal flow state until a baroclinically unstable meridional temperature gradient has been established, at which time eddies (simulated by a random generator) are introduced into the mean flow system. The equations then describe a flow system characterized by a system of baroclinic instability waves, subject to the imposed forcing functions.

The numerical technique used in the integrations was similar to that used by Everson & Davies (1970). An "Arakawa" type differencing scheme was applied to the non-linear advective terms to suppress non-linear numerical instability. A new scheme was developed to suppress error growth near the North and South boundaries, where an application of the Phillips type boundary conditions lead to non-conservative Arakawa Jacobians and consequent errors. This difficulty was avoided by setting the values of q' and ψ' (the deviations from the zonal mean values) to be zero along the rows next to the boundaries; the model was then found to retain a constant domain mean temperature corresponding to a zero domain mean heating (used in climate model studies). There was no loss of baroclinic activity and no spurious production of mean temperature, which was noted in the Everson and Davies model to be only a slow growth, but has to be avoided altogether in studies requiring very long time integration.

The "diffusive" and "stress" terms were expressed in finite difference forms and evaluated implicitly in initial integrations and centred in time as in previous computations. An important modification was then made in the time derivative formulation which led to a significant increase in computation speed which is of considerable importance in very long integrations. This was a modification of the Adams–Bashforth method.

If we write eq. (1) in the form

$$\frac{\partial}{\partial t} q_1 = f_1 \quad (9)$$

then values of q and f at successive time steps Δt can be related (see, e.g. F. Gerrald, 1970) in terms of forward difference operators of the form $\Delta f_\tau = f_{\tau+1} - f_\tau$ by

$$q_{\tau+1} = q_\tau + \Delta t(f_\tau + \tfrac{1}{2}\Delta f_{\tau-1} + \tfrac{5}{12}\Delta^2 f_{\tau-2} + \\ + \tfrac{3}{8}\Delta^3 f_{\tau-3} + \ldots) \quad (10)$$

We also have

$$\Delta f_{\tau-1} = f_\tau - f_{\tau-1}, \Delta^2 f_{\tau-1} = f_\tau - 2f_{\tau-1} + f_{\tau-2}$$
$$\Delta^3 f_{\tau-1} = f_\tau - 3f_{\tau-1} + 3f_{\tau-2} - f_{\tau-3}, \text{ etc.}$$

A first approximation to eq. (10) is then

$$q_{\tau+1} = q_\tau + \Delta t f_\tau$$

This is well known to be unsuitable for meteorological waves. The second approximation, taken to the first two terms in the brackets in (10), gives

$$q_{\tau+1} = q_\tau + \frac{\Delta t}{2}(3f_\tau - f_{\tau-1}) \tag{12}$$

Further successive approximations give

$$q_{\tau+1} = q_\tau + \frac{\Delta t}{12}(23f_\tau - 16f_{\tau-1} + 5f_{\tau-2}) \tag{13}$$

and

$$q_{\tau+1} = q_\tau + \frac{\Delta t}{24}(55f_\tau - 59f_{\tau-1} + 37f_{\tau-2} - 9f_{\tau-3}) \tag{14}$$

Approximations (12), (13), (14) were all tested in the model, the general characteristics of the time integration (e.g. eddy kinetic energy functions) were similar in all cases, computational stability was preserved using time steps of 30 min, with a forward time step taken every 30 model days.

The Adams–Bashforth schemes were tested with the implicit evaluation of stress terms replaced by conventional explicit evaluation. This allowed for the elimination of the complex inversion process used for obtaining the q values from the ψ values in the integrations; a considerable saving in computer time followed. This is of course of great benefit in theoretical climatic change studies. Single precision and double precision arithmetic computations were carried out to test rounding errors, but no model inconsistency revealed itself, and very small adjustments (made necessary by the unavoidable computational rounding errors) were automatically made at each time step to ensure that the prognostic variables obeyed certain conservation principles.

It was found by a series of model tests that the difference between the implicit time schemes used by, e.g. Everson & Davies (1970), and the new explicit schemes allied to the Adams–Bashforth time averaging schemes led to a doubling of the operational speed. The scheme, eq. (14), was used in the later investigations involving very long time integrations, when the Q_2 heating term is allowed to be model dependent. The effect of the use of the multiple time levels scheme at each time step was felt to be desirable also from a climate modelling point of view, since the extra time levels bring in more of the history of the flow at each time step.

This version of the model was found to be capable of producing about 140 days of model integrations in 10 min of computer time on an I.B.M. 370/195 computer.

Using these computer techniques, and the geographically fixed heating function, numerical experiments were made over 100 days periods, to find the "best" values, as defined by criteria (a) and (b), of the parameterization coefficients k_2, k_4, A, and λ. These are employed in the model to represent important processes that the model is unable to resolve, and since they are assigned fixed values throughout the integration their choice must be carefully made. A more realistic approach might be to relate their values to some aspect of above-grid scale model flow. However, as only planetary scale features of atmospheric flow are studied, simple parameterizations are initially adequate, particularly with the availability of limited computer usage. Numerical values used by Everson and Davies were tried, together with some neighbouring values, in a model with geographically fixed heating. The model was integrated for 120 days from day 0, using various values for k_4, A, and λ^2, and for 120 days from day 120 using various values of k_2, the effects of varying one parameter being studied whilst keeping the other three fixed at their previous levels. The following values were tested; (a) $k_2 = 0.05 \times 10^{-6}$, 0.25×10^{-6}, 0.50×10^{-6}, and 1.00×10^{-6}, sec^{-1}; (b) $k_4 = 0.5 \times (4 \times 10^{-6})$, $1.0 \times (4 \times 10^{-6})$, and $1.5 \times (4 \times 10^{-6})$, sec^{-1}; (c) $A = 0.1 \times 10^5$, 1.0×10^5, 1.5×10^5, and 10×10^5 m^2 sec^{-2}; (d) $\lambda^2 = 1.2 \times 10^{-12}$, 1.5×10^{-12}, 1.8×10^{-12}, and 2.0×10^{-12}, m^{-2}. The eddy kinetic energy functions, K', corresponding to each of these are given by Gordon (1975), the results for (a) and (d) being shown in Fig. 2, and are interesting in demonstrating the sensitivity of the model to changes in numerical values of the parameterization coefficients. A study of the computed K' functions and the computed surface flow and temperature patterns led to a best compromise choice of $A = 0.6 \times 10^5$ m^2 sec^{-2}, $\lambda^2 = 1.5 \times 10^{-12}$ m^{-2}, $k_2 = 0.5 \times 10^{-6}$ sec^{-1}, and $k_4 = 4.0 \times 10^{-6}$ sec^{-1}. These values together were also found to be convenient for the model's computational stability test criterion with its associated varying weight of computer usage. These numerical values were then applied in the version of the model which included a time dependent heating, and integrations were carried out over a very long time period up to 1800 days.

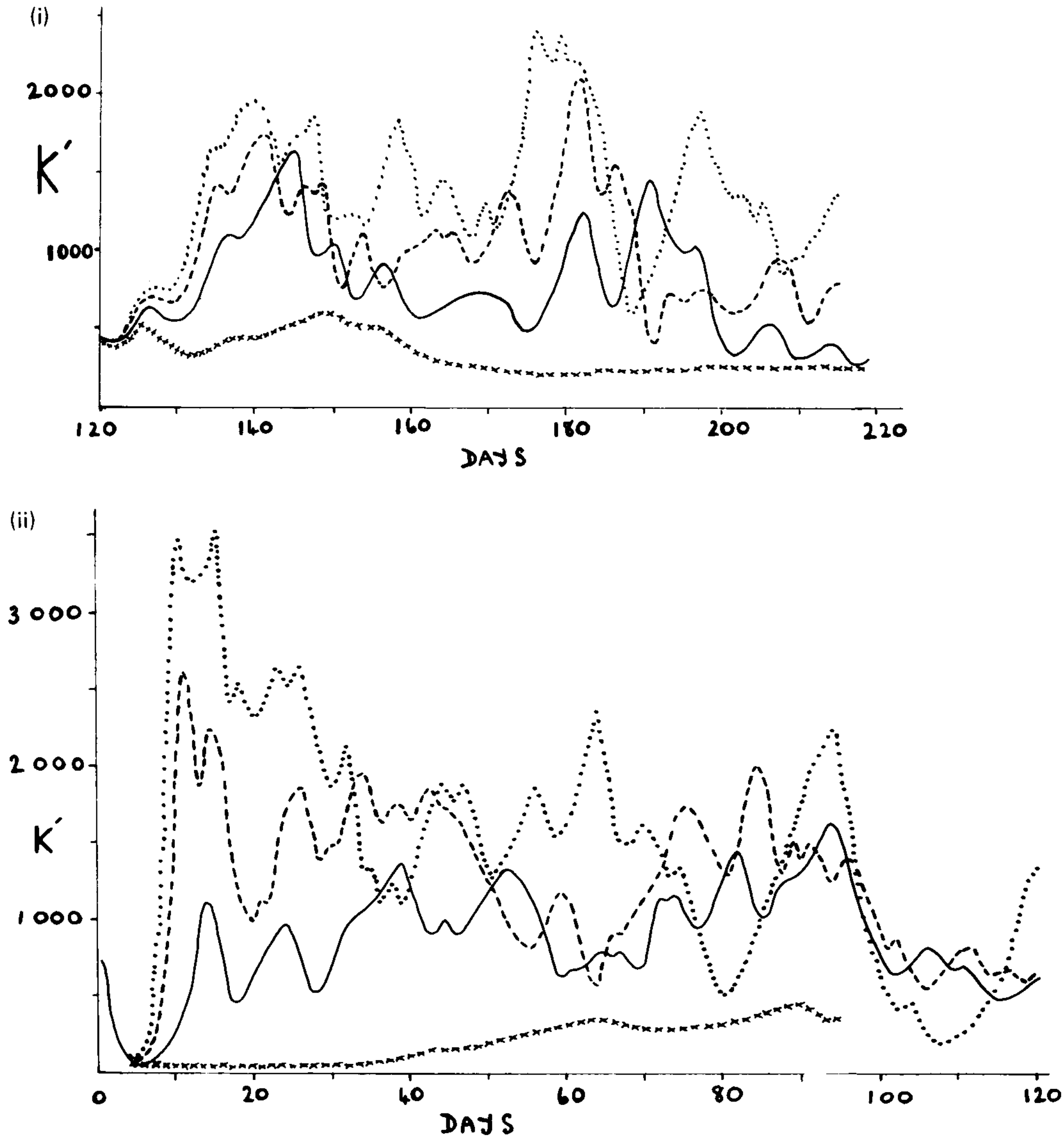

Fig. 2. Eddy kinetic energy function, K', in units, as defined by Phillips (1956): (i) ....., $k_2 = 0.05 \times 10^{-6}$; — — —, $k_2 = 0.25 \times 10^{-6}$; ——, $k_2 = 0.50 \times 10^{-6}$; ××××, $k_2 = 1.0 \times 10^{-6}$; all in units of sec^{-1}: $k_4 = 4.0 \times 10^{-6}$ sec^{-1}, $A = 0.6 \times 10^5$ m^2 sec^{-2}, $\lambda^2 = 1.5 \times 10^{-12}$ m^{-2}. (ii) ......, $\lambda^2 = 2.0 \times 10^{-12}$; – – –, $\lambda^2 = 1.8 \times 10^{-12}$; ——, $\lambda^2 = 1.5 \times 10^{-12}$; ×××××, $\lambda^2 = 1.2 \times 10^{-12}$; in units of m^{-2}; $k_2 = 0.5 \times 10^{-6}$ sec^{-1}; $k_4 = 4 \times 10^{-6}$ sec^{-1}; $A = 0.6 \times 10^5$ m^2 sec^{-2}.

4. Numerical experiments concerning changes of surface albedo distribution with changes of solar radiation

The model incorporating time independent heating was integrated for 320 days, and then restarted at day 230 using the new time dependent heating function and a 90-day run compared with the first model results. An inspection of model behaviour showed that the new model had accepted the variable heating function without any numerical difficulties: the surface flow patterns are similar with comparable baroclinic activity and a similar index cycle in K', apart from a tendency for the time dependent heating model to lag behind the other, due to the in-built, feedback dependence. It was therefore concluded that the time dependent heating model was a suitable one to carry out the extensive numerical experiments required. The general method of integration in this model involved the introduction of a variable surface albedo distribution by linking values of surface albedo to the model predicted surface temperature distribution, T_*, using the empirically linked dependence given by Smagorinsky (1963) based on analysis of data obtained from recent decades. At a given time in the integration the model temperature, T_2, at 500 mb would be predicted by solving eqs. (1) to (4) and the associated T_* deduced from (5): this carries with it a corresponding albedo distribution. If the predicted surface temperature at a given location was less than that given at the pole (for present day conditions) then the albedo value at that location was given the value at the pole, with a corresponding technique for temperatures in excess of the present maximum temperature in the tropics. A surface albedo distribution was consequently specified over the whole domain. The zonally averaged surface albedo distribution characteristic of recent decades is shown in Fig. 3 and clearly shows the effect of snow and ice cover at high latitudes. To use the surface balance eq. (5) exactly at all points in the domain, a complex, iterative scheme is strictly necessary. An initially predicted T_2 value leads to a T_* value and associated A_*; this leads to a new $\dot{Q}_2$ value and in turn a new T_2 value, etc. However, since the model uses time steps of 30 min, and since the albedo change often lags behind temperature changes in nature, then it was felt to be a reasonable approximation to use the albedo values from the previous time step in the surface balance equation in computing a close approximation to the surface temperature and the related T_2, giving $\dot{Q}_2$ for the next time step. This slight approximation was responsible for avoiding a considerable addition to the very heavy computing burden.

In the initial 90-day test integration of the time dependent heating model, the mean "ice-edge" (simulated by a specific A_* value from available data as described above) varied between latitudes 69° N and 72° N, finally settling down at about 71° N, the surface albedo distribution being very similar to present day values. However, since in the model the surface temperatures are obtained from the surface energy balance equation, these and the associated albedo values are required to adjust instantaneously to maintain the balance. This leads to changes in surface albedo values which are of course very much faster than in the real atmosphere. This process could have been slowed down by taking running averages of surface albedo over specified periods, e.g. a baroclinic index cycle, but this would have involved excessive demands on available computer capacity; it was felt to be not necessary in a first-order study of the effect.

The main aim of the investigation was to evaluate the latitudinal position of the mean asymptotic state, about which the albedo distribution oscil-

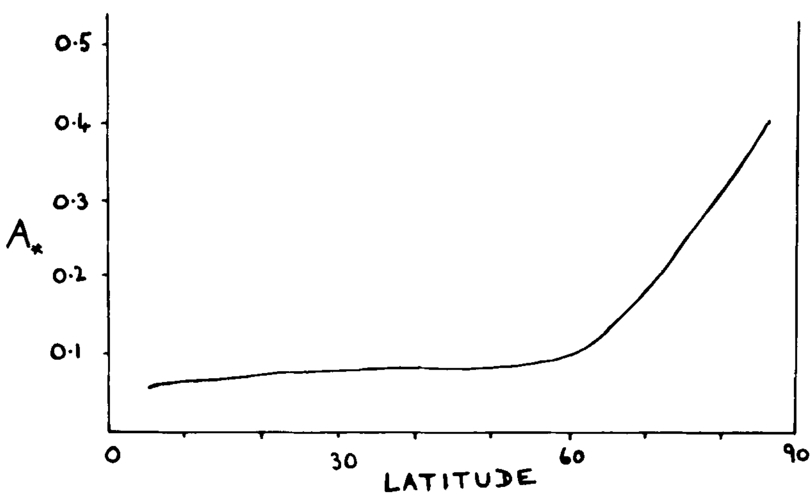

Fig. 3. Surface albedo, A_*, as a function of latitude, taken from Smagorinsky (1963).

Table 1

Sequence	Period of integrations (model days)	Type of heating function	Percentage reduction in S_0
A	1–127	$Q(\theta)$	0.0
B	128–460	$Q(T_2, T_*, A_*)$	0.0
C	461–720	$Q(T_2, T_*, A_*)$	0.5
D	721–1000	$Q(T_2, T_*, A_*)$	1.0
E	1001–1320	$Q(T_2, T_*, A_*)$	1.5
F	1321–1600	$Q(T_2, T_*, A_*)$	2.0
G	1261–1800	$Q(T_2, T_*, A_*)$	3.0

lates, corresponding to each solar radiation value, and to test the stability of each asymptotic state. It was not of course certain beforehand whether a specific asymptotic state exists (i.e. a transitive state), even in our relatively simple model, for each fixed external condition. The length of the time integrations between each successive reduction δS_0 of total solar radiation S_0 depended on (a) the time the model required to adjust to changes in S_0, and (b) the time taken for the results of the numerical integration to suggest that an asymptotic state had been reached.

The model was deemed to be in an asymptotic state under a time dependent heating when (a) the domain mean of the heating $[\dot{Q}_2]$ was oscillating about a zero value, with a long-term time average of zero, and (b) the surface albedo distribution had also reached a distribution that no longer changes in the long time period average.

The sequence of numerical experiments carried out are indicated for clarity in Table 1; this displays the type of heating function employed during each particular sequence together with the percentage reduction in force during that sequence. Sequence A was sufficiently long to allow the model state to move well away from initialization conditions.

Beginning with day 127, the model was changed from a fixed in time, latitudinally dependent heating function type to a fully self-determining heating function, dependent on model atmospheric temperature, T_2, together with the surface balance condition involving T_* and its associated A_*. The times at which changes were made in S_0 are shown in the Table, these changes being introduced in stages over one model day, up to 2% reduction. Although it is doubtful whether the premises of the model are likely to hold after this stage a final experiment was conducted in which the model was restarted at day 1260 (in sequence E, when a 1.5% reduction was in force) and the reduction in S_0 was increased to 3%.

The four model characteristics discussed in each sequence were (a) domain eddy kinetic energy, K', (b) zonally averaged zonal velocity at level 1, $\bar{u}_1$, (c) deviation of mean domain heating $[\dot{Q}_2]$ from zero, (d) zonally averaged surface albedo, $\bar{A}_*$.

4.1. *The K' variations*

A good indicator of the time variations in the structure of large-scale atmospheric flow and its associated index cycle is the domain integral of eddy kinetic energy, K'. In Fig. 4, the computed K' curves for the period of days 200–700 are shown to illustrate the characteristics of the results obtained over the whole 1800 day period: the changes in the external heating function S_0 occurring in this range are indicated by a vertical line. The results for the full period are given by Gordon (1975). The form of the variations seen in K' and in total energy E suggest that the model had fully adjusted to the initial conditions by day 120. By comparing the general nature of K' variations before and after day 127, the stage at which the time-dependent heating was introduced into the model, it was seen that the model behaviour was not unduly affected in general characteristics by the change. These general characteristics of the computed K' (amplitude and average period) are seen to be typical of atmospheric variations (see e.g. Smith, 1973). They are characterized by periods of fairly rapid changes in K' magnitude and other periods of much slower and larger amplitude oscillations, but the general characteristics of K' behaviour remained the same after each reduction in S_0 at days 460, 720, 1000 and 1320.

It was interesting to note that there were periods

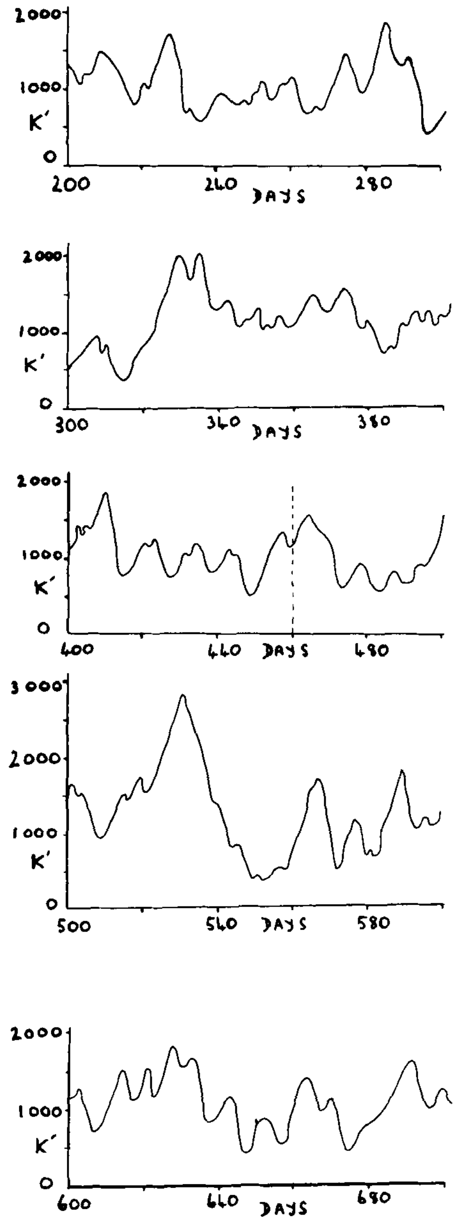

Fig. 4. Eddy Kinetic energy function K' (units as defined by Phillips, 1956) as a function of time of integration in model days from day 200 to 700; the vertical broken line indicates a change of 0.5% made in solar radiation S_0.

of very large K' values at the following day numbers, the associated K' values being given in parentheses; 330 (2050), 530 (2800), 740 (1950), 990 (2200), 1120 (2400), 1310 (3550), 1390 (2200), 1540 (1700), 1660 (2800), and 1755 (1850). It was noted that at some, but not all, of these maxima there were fundamental changes in the overall behaviour of the model jet streams; these were clearly seen by plotting the variations of $\bar{u}_1$, the zonal means of zonal velocity at level 1, and they indicate sudden changes in the general characteristics of general circulation behaviour. Following these times of very large K' values, there were often seen to be periods of smaller than average K' values. This is due to the large baroclinic activity (associated with large K' values) having substantially reduced the atmospheric Equator to Pole temperature gradient, and there then follows a quiet period until the temperature gradient is built up again.

4.2. *The $\bar{u}_1$ variations*

Analysis of the zonally averaged zonal wind at 250 mb, $\bar{u}_1$, turned out to be unexpectedly interesting. The $\bar{u}_1$ variations with time are shown in Fig. 5 for days 200–600, and illustrate the typical variation in structure of the whole 1800-day period of integration, the contours of $\bar{u}_1$ being plotted at 10 m/sec, intervals. These charts show that the main jet stream has a value of about 50 m/sec and throughout the whole period the main jet is seen to move meridionally in a fairly regular manner between about 35° and 65° latitude. As the main jet moves south it absorbs any minor jet positioned to the south of it and often leaves room for the development of a minor jet to the North. Then it subsequently moves North, the minor jet to the North of it being reabsorbed, and a minor jet then forms to the South.

Inspection of jet stream behaviour at times of peak K' values revealed the unexpected result that at some of these days (day 530, 1120, 1310) there were *sudden, complete* alterations in the jet stream behaviour, causing also sudden alterations in other aspects of model flow. This phenomenon had not been previously noted in shorter period integrations. Prior to each of these changes of mode, the main jet is at its most Northerly position and the minor jet to the south is well developed. Taking the model day period 535 to 540 as a specific example, it is seen from the figure that the K' behaviour before day 510, say, is typical of the average changes over the 1800-day range. By day 530, however, the K' value has increased to twice its normal value. The main jet is seen to move from its most Northerly position at day 400 to a

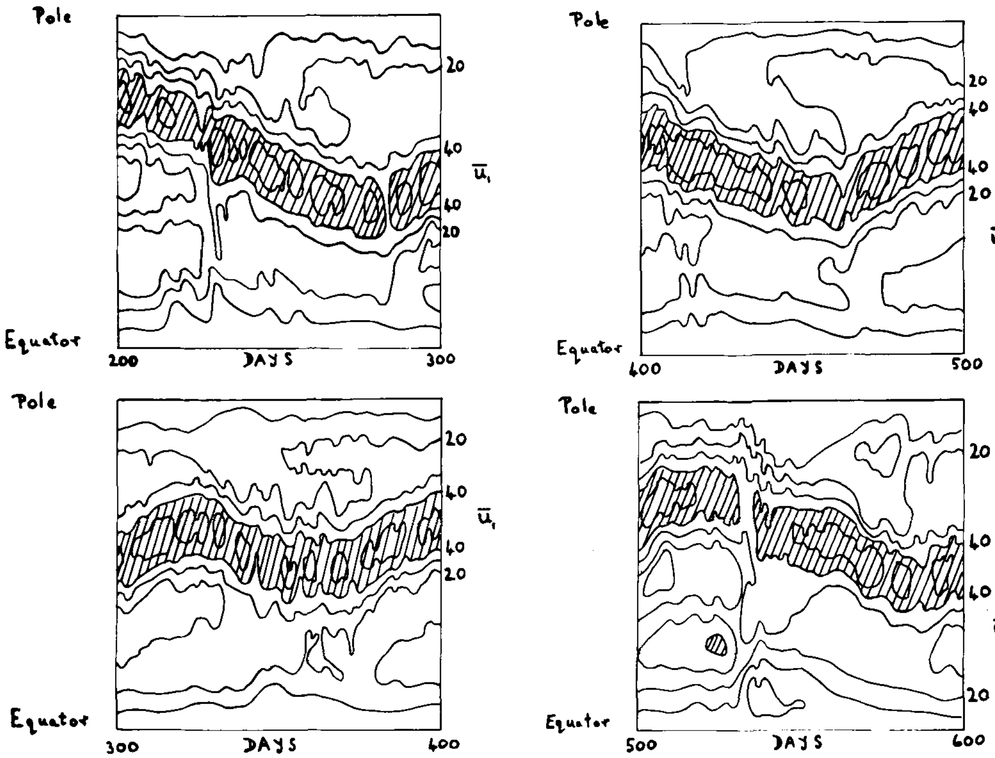

Fig. 5. $\bar{U}_1$ in m/sec: latitudinal distribution of zonally averaged 250 mb, zonal wind component shown as a function of time for days 200–600. The jet stream region, defined by $\bar{U}_1 \geq 40$ m/sec, is shown shaded.

southerly position by day 460; it then moves steadily North up to day 510, when it reaches its most Northerly position again and persists at latitude 65° N for about 15 days with a value of about 55–60 m/sec. At the same time the southerly minor jet stream has attained a value of over 40 m/sec at latitude 25° N. These two jets then combine in a very short time at around day 535, and by day 550 the single jet is positioned at about 55° N with a value of 50 m/sec and then moves quickly south, resuming the usual main jet behaviour. A study of the zonal kinetic energy for the whole domain, $\bar{K}$, is particularly revealing. As shown in Fig. 6, there is a rapid loss of $\bar{K}$ value due to conversion of $\bar{K}$ to K'. This is typical of *barotropic* instability and clearly has a crucial and remarkably sudden effect on large-scale flow characteristics. This phenomenon occurred also at days 1125 and 1305 with similar general characteristics. In both cases the main jet was at its most Northerly position, just beginning to move South and the minor jet to the South is fully developed. It was, however, noted that the *sudden* combination of the two jets does not take place each time the main jet begins to move South from its most Northerly position. A comparison of the general characteristics of these occasions is shown in Table 2, and Fig. 7 shows the sudden change in surface flow pattern by comparing the flow before the change, at day 530, with the flow after the change, at day 560.

The criteria for sudden changes and sudden combinations of the main and minor jet streams appear to be as follows. (a) The main jet must exceed 50 m/sec in speed and be positioned at an extreme Northerly position of 60° to 70° latitude. (b) The minor jet must have a velocity of over 40 m/sec at about 25° to 30° latitude. (c) The minimum zonal velocity between these latitudes at about 40° to 50°, must be less than 10 m/sec. These results suggest that a major criterion is that a large-scale meridional shear of zonal flow must exceed some critical value to produce this planetary scale barotropic instability effect in the model. It

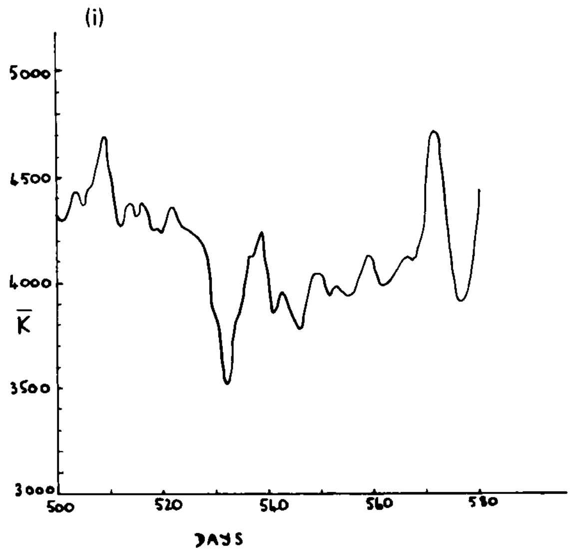

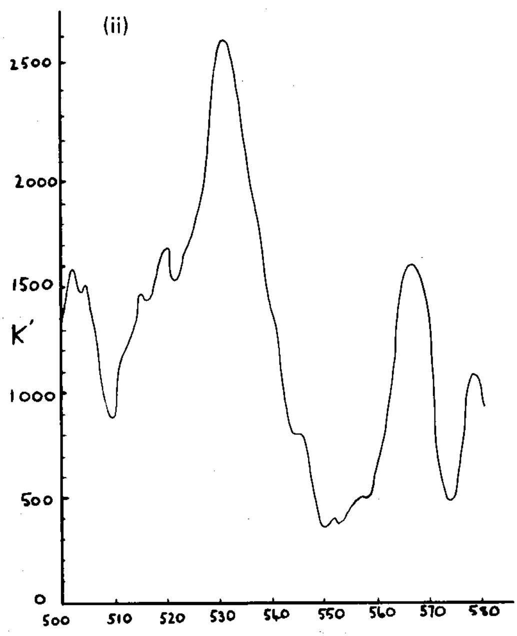

Fig. 6. (i) Zonal Kinetic Energy, $\bar{K}$, as a function of time of integration from day 500 to day 580. (ii) Eddy Kinetic Energy K', over the same range: in units defined by Phillips (1956).

Table 2

Day	Main jet Velocity m/sec	Main jet Latitudinal position ° North	Minimum flow Velocity m/sec	Minimum flow Latitudinal position ° North	Minor jet Velocity m/sec	Minor jet Latitudinal position ° North
90	60	60	10	40	35	25
205	55	55	5	45	35	25
330	50	55	20	35	30	20
405	55	60	10	35	30	20
535	55	65	10	45	40	25
620	60	55	20	30	25	20
760	60	65	5	45	35	25
865	55	55	10	35	30	20
970	55	60	10	45	30	30
1125	50	60	10	45	40	30
1300	50	70	10	50	40	30
1460	40	65	10	45	40	30

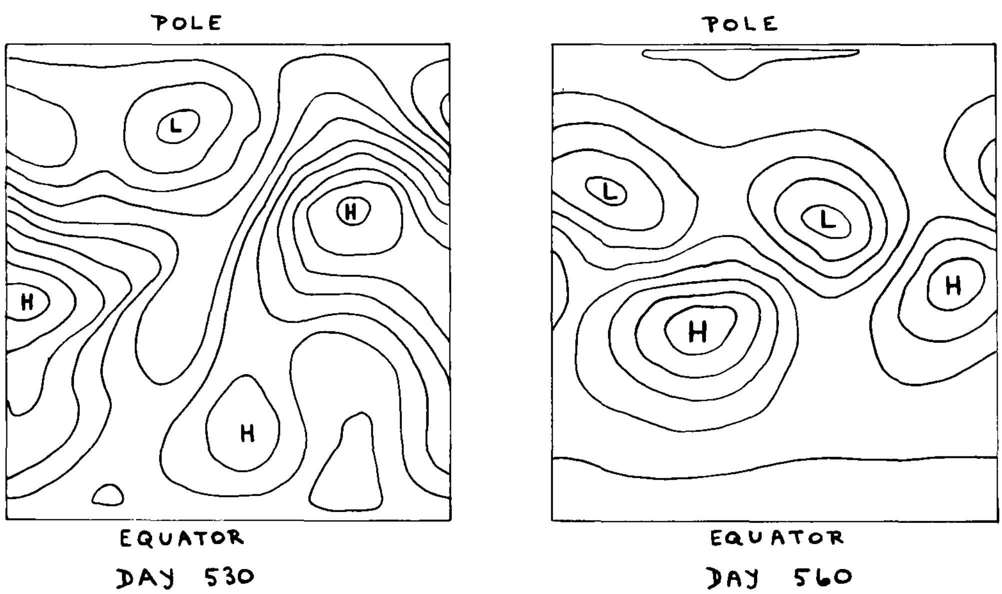

Fig. 7. Surface Flow Patterns at day 530 and at day 560 indicated by 1000 mb contours at 100 ft intervals.

also strongly influences the temperature distribution, and the surface albedo distribution and is related to the formation of blocking anticyclones. It was noted, by e.g. Everson & Davies (1970), that a sufficiently strong E–W temperature contrast, at times of low K', could lead to the formation of these systems in a numerical model: this was verified by Smith (1973) from an analysis of observational data. In the present model there is no forced land–sea heating contrast, but a strong E–W surface temperature gradient is occasionally produced through the moving albedo distribution.

It is consequently a phenomenon which could be of importance in the dynamics of climatic change and clearly requires further detailed investigation.

4.3 *The domain mean heating*

The domain mean atmosphere heating in the model, $[\dot{Q}_2]$, gives us a criterion to determine whether the model has reached an asymptotic state for a given set of external conditions. When $[\dot{Q}_2]$, is plotted against time, it gives an indication of the existence of an asymptotic state (as previously defined in this section), if $[\dot{Q}_2]$ makes small oscillations about a zero mean: it also gives the time taken to approximate to such a state. The associated mean latitudinal position of the zonally averaged surface albedo distribution, A_*, is, of course, crucial in determining the mean position of a simulated "snow–ice" edge.

Typical variations of $[\dot{Q}_2]$ with time are given in Fig. 8 for (i) day 400 to 700, (ii) day 1200 to 1500; changes in external heating are shown by vertical lines. At day 460, e.g. S_0 was reduced by 0.5% everywhere, causing $[\dot{Q}_2]$ to become negative immediately. This of course, was due to the reduced solar heating and there was no longer a balancing of mean outgoing radiation. The negative $[\dot{Q}_2]$ state lasted for about 100 days, after which $[\dot{Q}_2]$ began to oscillate around a zero value, indicating strongly the existence of an asymptotic zero domain mean heating mode, the model having readjusted its surface albedo distribution with the consequent feedback effect on the heating. Similar events followed each successive reduction in S_0 value, suggesting *model* transitivity. It was noted that as the reduction in S_0 was increased, the time which the model took to re-adjust, with a new spatial distribution of surface albedo, increased and this distribution moved southwards appreciably. The *amplitude* of the $[\dot{Q}_2]$ fluctuations also naturally increased. The model expressed a tendency, for the larger reductions, to overcool; the negative feedback dependence of the heating on atmospheric temperature then leads to an excess of heating, and the process is reversed progressively until an asymptotic situation is approached, with its associated small oscillations characteristic. Hence the positive feedback of surface albedo and negative feedback of atmospheric temperature appear to be over-correcting initially for larger S_0 reductions, indicating a less stable situation as these are increased.

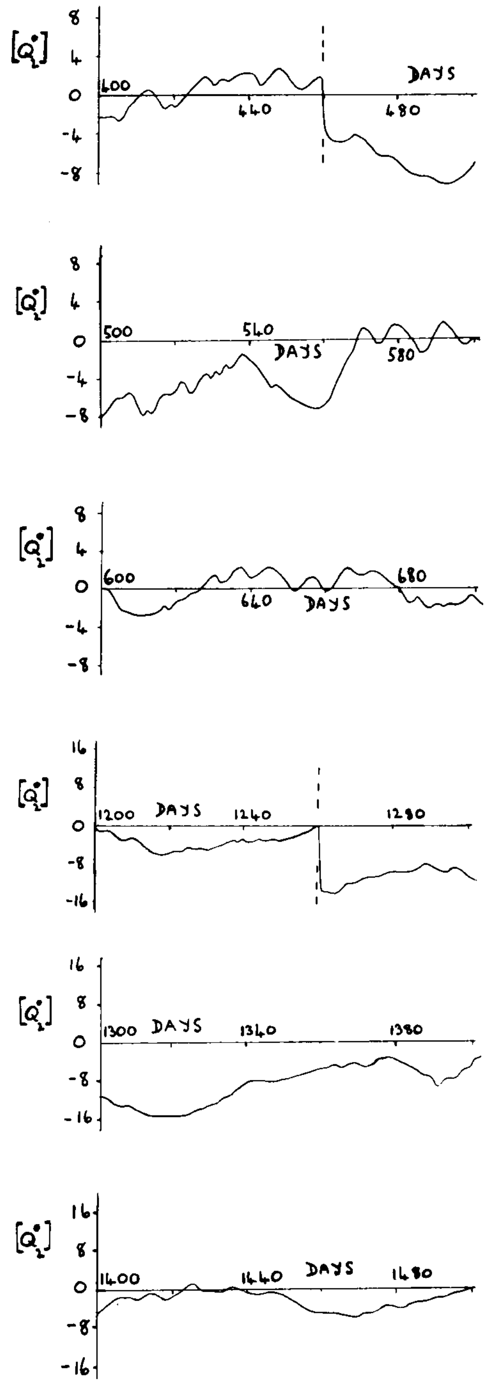

Fig. 8. Integrated Domain Heating, $[\dot{Q}_2]$, shown as a function of time of integration. (i) Days 400–700: (ii) Days 1200–1500. The vertical broken lines indicate changes made in Solar radiation S_0.

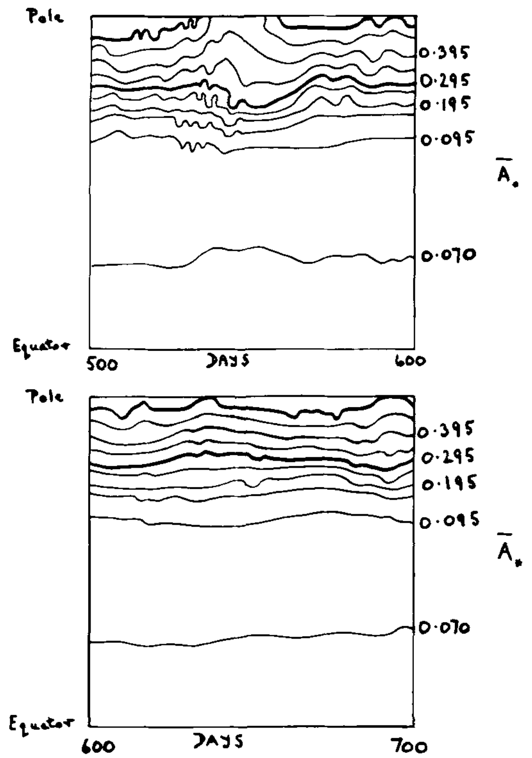

Fig. 9. Latitudinal Distribution of zonally averaged surface albedo, $\bar{A}_*$, as a function of time, plotted at 0.070 and at intervals of 0.050 from 0.095 to 0.445, for days 500 to 700.

4.5. *The surface albedo changes*

The response of the A_* distribution to change in solar radiation is clearly of prime importance in a climate model and is a sensitive indicator of the stability of the model. In order to give an indication of the type of distribution encountered in the integration, the $\bar{A}_*$ distribution (i.e. the zonally averaged albedo distribution) as a function of latitude and of time is given in Fig. 9 for days 500 to 700, which includes one of the sudden changes. The albedo values, from zonally averaged data, vary from 0.070 at the equator to 0.480 at the Pole. The contours shown, from South to North, are 0.070, then 0.095 to 0.445 in steps of 0.05, with a final contour of 0.478. The contour $A_* = 0.295$ (shown as a heavy line) is taken to represent approximately the mean latitudinal position of the model "snow–ice" edge. This is, of course, of no physical significance to our model, since the surface albedo values have a continuous spatial distribution: the "ice" edge contour allows the overall temporal movement of the distribution to be characterized.

For an asymptotic state we require the albedo distribution to oscillate about a mean distribution. The A_* value which was seen to oscillate about the 72° latitude (taken as the mean approximate position of the "ice" edge), after the model had been operating for several hundred days, was 0.295, and was taken as representative of the model "ice" edge. We note that the A_* values employed (related directly to computed T_* model values) are those given by Smagorinsky (1963) and represent values, which are based on averages over land and sea, and are continuous across the model "ice" edge limit. Jet stream movements were found to cause large heat re-distributions in the model and were reflected in the associated rapidly changing A_* distributions. Prior to the sudden changes of jet stream mode, the A_* distribution enters a period of considerable oscillation but after the "sudden event", it is seen to settle down to a relatively uniform movement. As examples of the A_* distribution over the whole domain, contours of equal albedo values are given in Fig. 10 for day 530 (before the event) and for day 560 (after the event). The model assumption of instant response of A_* to T_* changes exaggerates the rate of movement of A_*. An averaged response method was not attempted in a first approach to the problem, due to computer limitations.

The main aim of the investigation was to calculate (a) the latitudinal position of the mean zonally averaged model "ice edge" for a sequence of reductions δS_0 in S_0 up to 3% and to compare with our results, Gordon & Davies (1974), obtained, using a modified Budyko, statical, energy balance method and (b) to test the sensitivity of these successive positions. The model "ice edge" was plotted out for each day in the 1800 day integration. Typical values are shown in Fig. 11 for (a) days 250–400 ($\delta S_0 = 0$), (b) days 850–1000 ($\delta S_0 = 1\%$), (c) days 1150–1300 ($\delta S_0 = 1.5\%$), and (d) days 1650–1800 ($\delta S_0 = 3\%$).

For 0.5% reduction in S_0 there is little movement of the "ice edge" southwards; for a 1% reduction, from day 720 to day 1000, the movement to the South becomes noticeable, with the final position at around 70.5°. In the 1000- to 1320-day period with 1.5% value for δS_0 it reached 65° at times, following a jet stream sudden change at day 1120. With a 3% reduction the final mean

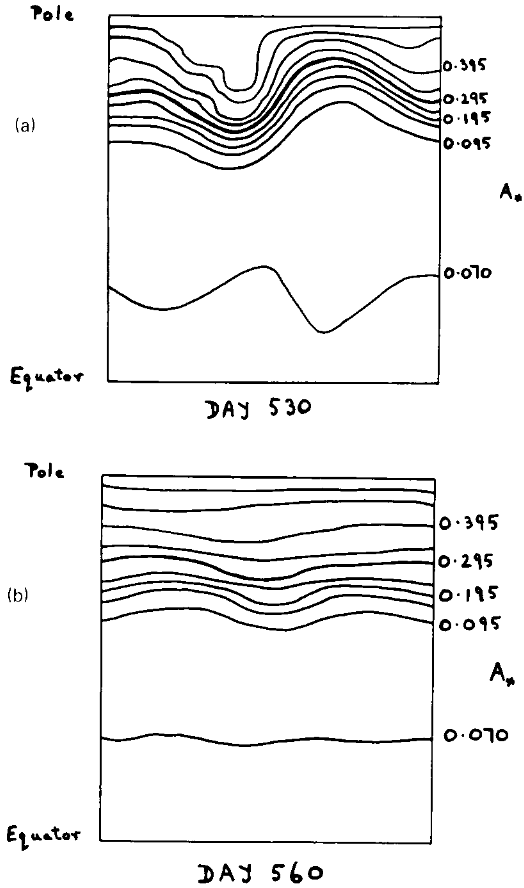

Fig. 10. Spatial Distribution of surface albedo, A_*; (a) at day 530, (b) at day 560, plotted at 0.070 and at intervals of 0.050 from 0.095 to 0.495.

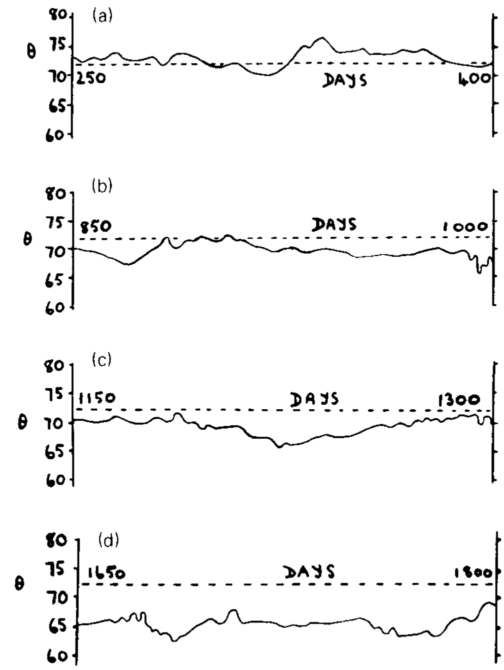

Fig. 11. Zonally averaged "ice" edge latitudinal position, θ, shown as a function of time of integration. (a) days 250–400, ($\delta S_0 = 0$); (b) days 850–1000, ($\delta S_0 = 1\%$); (c) days 1150–1300, ($\delta S_0 = 1\frac{1}{2}\%$); (d) days 1650–1800, ($\delta S_0 = 3\%$).

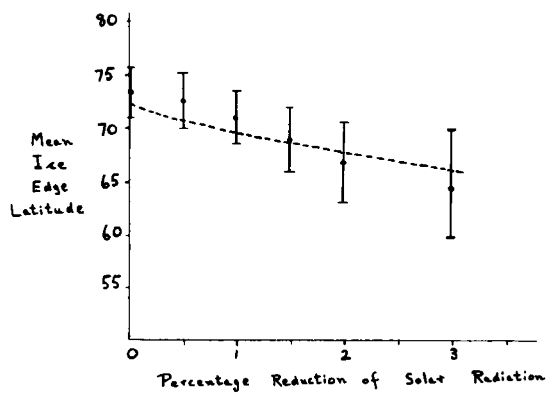

Fig. 12. Zonally averaged Ice Edge Latitudinal Position; as a function of percentage reduction of solar radiation; --------- calculated by the statical (Budyko) energy balance method; . . . . ., calculated by the time-dependent model. I indicates amplitude of oscillation of the "edge".

position of the "ice edge" was at about 65° but with a much larger degree of movement to the North and South of this mean position (sometimes as far South as 60°): this indicates an increasing tendency to instability in the sense of increasing amplitude, but there was no sign of climatic collapse. This instability tendency is partly explained by the negative feedback' of the atmospheric temperature T_2 on the atmospheric heating, opposing the positive feedback of the extra "snow–ice cover", and partly by the fact that the higher albedo values are now entering the region of greater baroclinic activity of the model, i.e. the tracking centre of the mid-latitude cyclonic systems.

In Fig. 12, the Mean Ice Edge Latitude is plotted against Percentage Reduction of Solar Radiation. The movement to the South of the mean latitudinal position of the edge is clearly seen, and it is interesting to note that these results approximate quite closely to the values previously calculated by Gordon & Davies (1974) using a modified Budyko energy balance method, although the gradient of the time dependent heating model result is steeper than that based on the Budyko method and suggests that at higher reductions the time dependent model would give a more rapid movement to the equator. The results shown in Fig. 12 also show the rapidly widening amplitude of movement of the "ice edge" with its associated indication of approaching instability as δS_0 is increased. Although it was thus found that the 3% reduction was not sufficient to trigger off climatic collapse (in the sense of a movement of ice to low latitudes), a Southward fluctuation could be sufficient to cause a movement in the A_* distribution, which if reproduced in the atmosphere might become irreversible.

5. Conclusions

The main results of the numerical experiments using a time dependent heating, and albedo moving, model are as follows:

(i) The mean latitudinal positions of the simulated "ice edge" (expressed only in terms of a specific surface albedo value), corresponding to a sequence of values 0.5, 1.0, 1.5, 2.0, 3.0% reductions in solar radiation, are similar to those previously calculated by Gordon & Davies (1974) using a statical energy balance method (of Budyko type).

(ii) It is seen that as these reductions in solar heating increase and approach 3%, the spatial amplitude of oscillation of the "ice edge" also increases sharply, suggesting the approach of climatic instability.

An interesting by-product of the study concerned the behaviour of the model jet streams. On a small number of specific occasions during the 1800-day period of integration, a frequently occurring double jet stream collapses into a single jet, with an accompanying rapid transfer of energy from zonal to eddy form, characteristic of *barotropic* instability. This occurred when the N–S zonal velocity shear was at its peak value. This may be a phenomenon of importance in climate change dynamics and requires further study.

In further developments of the model a number of thermodynamic and dynamic factors will require refinement in order to determine their effects on planetary scale dynamics. For example, spatial and temporal variations of static stability, λ, and representations of vertical eddy transfer of heat need to be inserted and compared with the results of the present model, in which we have chosen a domain average numerical value for λ in order to satisfy the criteria of (a) realistic domain eddy kinetic energy functions, and (b) realistic synoptic surface flow patterns. An important large-scale feature also to be inserted and explored is the contribution to the dynamics of climate of standing waves produced by planetary scale mountain barriers.

A key question for further studies with a higher order model is of course to see whether a system including a land–sea thermal differential will produce similar results to those of the present model. It is not clear whether such a system would do so, despite the possibly conservative effect of oceanic heating. In particular we note that the present model is based on *annual* and *zonally* averaged background data. The use of winter time Northern Hemisphere background conditions with the same S_0 reductions could well lead to more drastic results with the "ice" penetrating further South over the extensive land masses; succeeding summer heating conditions might well not be sufficient to return the ice to its initial stage, and so in a relatively small number of years produce a mid-latitude ice age.

6. Acknowledgments

H. B. Gordon gratefully acknowledges the financial aid of a S.R.C. (U.K.) Studentship and a N.E.R.C. (U.K.) Research Assistantship. We are also grateful for the assistance of staff at the Atlas Computer Laboratory, Chilton, U.K.

REFERENCES

Budyko, M. J. 1969. The effect of solar radiation variations on the climate of the earth. *Tellus 21*, 611–619.

Everson, P. J. & Davies, D. R. 1970. On the use of a simple two-level model in general circulation studies. *Q. J. R. Met. S. 96*, 404–412.

Gal-chen, T. & Schneider, S. H. 1976. Energy balance climate modelling: comparison of radiative and dynamic feedback mechanism. *Tellus 28*, 108–121.

Gerald, C. P. 1970. *Applied numerical analysis*. Addison-Wesley Pub. Co., London.

Gordon, H. B. 1975. An investigation into climatic change using mathematical numerical models. Ph.D. Thesis, University of Exeter, U.K.

Gordon, H. B. & Davies, D. R. 1974. The effect of changes in solar radiation on climate. *Q. J. R. Met. S. 100*, 123–127.

Gordon, H. B. & Davies, D. R. 1975. Mathematical prediction of climate change. *Nature 253*, 419–420.

Phillips, N. 1956. The general circulation of the atmosphere; a numerical experiment. *Q. J. R. Met. S. 82*, 123–164.

Schneider, S. H. & Dickinson, R. E. 1974. Climate Modelling. *Reviews of Geophysics and Space Physics 12*, 447–493.

Searle, J. W. & Davies, D. R. 1974. The sensitivity of dependence of large scale flow characteristics in a four-level model atmosphere on a simulated planetary boundary layer. *Tellus 27*, 145–154.

Smagorinsky, J. 1963. General circulation experiments with the primitive equations. *Mon. Wea. Rev. 91*, 99–164.

Smagorinsky, J. 1974. Global atmospheric modelling and the numerical simulation of climate. *Weather and Climate Modification*. J. W. Wiley, and Sons.

Smith, R. F. T. 1973. A note on the relationship between large scale energy functions and characteristics of climate. *Q. J. R. Met. S. 99*, 693–704.

ЧУВСТВИТЕЛЬНОСТЬ РЕАКЦИИ КЛИМАТИЧЕСКИХ ХАРАКТЕРИСТИК В ДВУХУРОВЕННОЙ МОДЕЛИ ОБЩЕЙ ЦИРКУЛЯЦИИ К МАЛЫМ ИЗМЕНЕНИЯМ СОЛНЕЧНОЙ РАДИАЦИИ

Построена двухуровенная квазигеострофическая модель общей циркуляции на β-плоскости, включающая зависящее от времени уравнение баланса энергии на поверхности и зависяшую от времени функцию нагревания на уровне 500 мб с соответствующими обратными связями. Эта система позволяет находить распределение температуры на поверхности земли в зависимости от времени, откуда можно получить переменное распределение альбедо поверхности, включая границу "снегового и ледового" покрова. Затем, с помощью численных экспериментов, проводимых на долгие сроки, изучается влияние последовательных малых изменений солнечной радиации (на 0,5% вплоть до 3%). Эти сроки достаточно длинны (полное время интегрирования 1800 модельных дней) для того, чтобы вызвать колебания в функции нагревания и распределении альбедо около их асимптотических средних величин. Последовательные широтные положения края "снега и льда" приблизительно согласуются с результатами расчетов Гордона и Дэвиса (1974), использовавших модифицированную форму метода статического баланса энергии Будыко (1969). Однако эксперименты также показывают, что чем больше уменьшение солнечной радиации, тем больше амплитуда пространственного перемещения в распределении альбедо, что указывает на сильную тенденцию к неустойчивости положения края покрова по мере приближения уменьшения радиации к 3%.